

VideoAFM—a new tool for high speed surface analysis

Jamie K. Hobbs,^{*a} Cvetelin Vasilev^a and Andrew D. L. Humphris^b

Received 8th August 2005, Accepted 21st October 2005

First published as an Advance Article on the web 11th November 2005

DOI: 10.1039/b511330j

The VideoAFM provides a 1000 fold increase in image rate compared to conventional atomic force microscopes, giving nanometre resolution images of surfaces at a rate of 15 frames s⁻¹, which is approximately 1 million pixels s⁻¹. Images of high stiffness surfaces such as calibration grids are provided for the first time, and allow for a more rigorous examination of the meaning of the data obtained with the VideoAFM. Instrumental changes that could provide true topographic images are discussed. The advantages of a high speed scanning technique that is integrated within a conventional AFM are outlined. Particular emphasis is given to the capability to 'tile' images, and hence rapidly map large areas with nanometre resolution. It is found that the inherent increase in stability that comes from a high frame rate leads to the possibility of manually manipulating the sample while maintaining a sharp image, allowing real-time user interaction with the AFM. The possible application of the VideoAFM approach for the very rapid analysis of surface properties and, ultimately, surface chemistry is discussed and some possible routes are given.

Introduction

Since its invention in 1986,¹ the atomic force microscope (AFM) has revolutionised the study of surfaces at the nanometre scale. The technique uses a sharp (~ 10 nm radius) probe tip mounted on a soft (0.01 – 50 N m⁻¹) cantilever to monitor the local interaction force at a point on the surface. The probe is then raster scanned relative to the surface, typically using a piezoelectric scan stage, so as to build up an image of the surface. Although initially developed as a tool for topographic mapping, a whole range of different contrast mechanisms were soon developed including magnetic force microscopy (MFM),² electric force microscopy (EFM)³ and friction force microscopy (FFM),⁴ to name but a few. The AFM is now also frequently used as a platform for other related measurements of surface properties, in which the base microscope acts as a method for tracking a local probe over the surface under study with nanometre accuracy, the probe itself being fashioned so as to make some other measurement of the local properties of the surface as it is scanned, for example thermal properties,⁵ magnetic properties⁶ or optical properties.⁷

As a tool for the analysis of surface composition and chemistry, several forms of the microscope have proved particularly successful. Friction force microscopy allows the quantitative measurement of the frictional force between a point asperity (the tip) and a surface. By controlling the surface chemistry of the tip, for instance through the application of a self assembled monolayer of known end group functionality, a map of the surface can be generated in which local variations in the interaction are high-lighted.⁸

This is particularly powerful if the surface is a mixture of two contrasting species of known chemistry but unknown distribution on the surface. A second technique which similarly measures local changes in mechanical properties of the surface is the phase imaging AFM. Here the cantilever on which the tip is mounted is oscillated at or close to its resonant frequency and variations in the phase difference between the drive force and the cantilever response are monitored. The resultant phase shift is related primarily to changes in the dissipative properties of the surface.⁹ Again, if the tip is functionalised in some way, it is possible to use this approach to map changes in the interaction with the tip over the surface and hence identify different regions of the surface. This approach has been taken to the extreme where an antibody is grafted to the tip so variations in probe-sample interaction correspond to the distribution of the complementary antigen on the sample surface.¹⁰

Despite the wealth of new information that has been obtained with these techniques, the approach itself is severely limited in speed. A typical AFM image of a surface with 256 by 256 pixels takes at least tens of seconds, and often minutes, to collect. Considering the high spatial resolution (~ 10 nm) that is a principal strength of the technique, it is clear that mapping large areas of a surface can be particularly laborious. An advantage of AFM compared to other high resolution techniques is its non-destructive nature—the surface is typically not damaged by the process of imaging and does not require staining or labelling in any way—which allows processes to be followed *in-situ* in real time, and often in their native environment (for instance biological processes under buffer solution). However, again, the slowness of the technique has severely limited the range of processes that can be accessed.

There are two main reasons for the limited speed of conventional AFMs. Firstly, the sharp tip and cantilever on which it is mounted have to be raster scanned relative to the surface with sub-nanometre accuracy. Typically this is carried

^aDepartment of Chemistry, University of Sheffield, Brook Hill, Sheffield, UK S3 7HF. E-mail: jamie.hobbs@sheffield.ac.uk

^bInfinitesima Ltd., Oxford Centre for Innovation, Mill Street, Oxford, UK OX2 0JX

out using piezoelectric devices, which are relatively massive and hence have resonant frequencies of 100s of Hz. This means that the maximum scan rate is limited to a few 10s of Hz before the scanner resonance is excited and the device becomes unstable, giving a maximum image rate of 10s of seconds (assuming 256 lines in an image). To address this issue, the stiffness of the scan stage can be increased, increasing its resonant frequency and hence the maximum line rate.^{11–13} Secondly, in most modes of operation an electronic feedback loop is used to control the position of the tip relative to the surface so as to keep the monitored interaction constant. This feedback loop has a time constant associated with it, both due to the electronics and again because of the inertia of the scanner, which has to be overcome for motion in the *z*-axis (conventionally taken as perpendicular to the sample surface). Indeed, in many cases the cantilever itself is taken to have an inherent response time as, if it is to behave as a Hookeian spring, it cannot be asked to respond at frequencies greater than its resonant frequency (typically several tens of kHz). To address this limitation, efforts have been made to reduce the mass of the object being moved in the *z*-direction,^{14,15} leading to the incorporation of a piezoelectric element within the cantilever itself.¹⁶

Recently we have developed a new form of AFM, the VideoAFM, which overcomes both of these limitations in a novel way.¹⁷ The conventional scanner is replaced with a micro-resonator (a quartz crystal tuning fork) that runs at its resonant frequency (~ 20 kHz) to provide the fast scan axis of the microscope.¹⁸ This provides a scan-stage that scans at 20 000 lines a second, compared to ~ 2 lines a second with a conventional AFM. Secondly, the cantilever has been redesigned to incorporate a passive method of maintaining tip-sample contact allowing a pixel rate of MHz. This leads to a microscope capable of obtaining a 256 by 256 pixel image in less than 35 ms. In this paper we will explore the capabilities of the instrument for the rapid analysis of nanometre scale variations in surface properties, the meaning of the pseudo topographical images obtained by the technique, and discuss the possible directions for future development as an analytical tool through the incorporation of different imaging modes.

Experimental method

An Infinitesima Ltd. (Oxford, UK) VideoAFM was used in conjunction with a conventional AFM, a Veeco Instruments Dimension 3100 with Nanoscope IV controller. The experimental set-up of the VideoAFM is given in ref. 17. The sample is mounted on a glass or silicon cube of 800 μm dimension that is in turn mounted on one leg of a micro resonant scanner. A similar cube is mounted on the other leg to balance the mass change of the resonator. The micro-resonator is mounted on a conventional single axis piezo that provides the slow scan axis, which is driven at a frequency that corresponds to the image rate (typically 15 Hz) as only the up or down scan is collected. Cantilevers were provided by Infinitesima (part no.s VC100.130 and VC100.131) with nominal stiffnesses of 0.01–0.03 N m^{-1} . The cantilevers are mounted in the conventional cantilever holder and their deflection monitored by the conventional deflection detection optics. As the

Dimension is a tip scanned device, this set up allows for both conventional and high speed imaging of the sample surface. The raw optical signal from the Dimension is fed into the Infinitesima VideoAFM Workstation where it is corrected in real-time for the sinusoidal distortion caused by the use of a resonator as a scan stage, processed and displayed to give a real-time video-rate image of the sample surface.

Two different samples were used. A sample of polyethylene oxide (M_w 220 kg mol^{-1} , M_w/M_n 1.1) was dissolved in toluene and solution cast onto a glass cube, heated to 90 $^\circ\text{C}$ to melt the sample, and then allowed to crystallize on rapid cooling to room temperature. The ensuing semicrystalline morphology is a mixture of spherulitic and dendritic structures, depending on the sample thickness. A silicon test grid was also provided by Infinitesima (an 800 μm cube with an etched surface consisting of 600 nm etched pits, 60 nm deep, separated by 660 nm and originally sourced from Nanosurf, part no. BT01994).

Results and discussion

Fig. 1 shows a VideoAFM image of a silicon calibration grid and the corresponding conventional AFM contact mode image of the same grid. The VideoAFM image was collected in 33.3 ms at a rate of 15 frames s^{-1} (only every alternate frame is collected) with an average tip velocity of 11 cm s^{-1} , compared to 85 s for the conventional AFM image with a tip velocity of 24 $\mu\text{m s}^{-1}$. Fig. 2 shows a VideoAFM image and the corresponding conventional contact mode image of a quartz crystal surface (the sample free micro resonator leg). These are the first AFM images of hard, non-polymeric materials obtained with tip velocities greater ~ 1 cm s^{-1} .¹²

The topographic information within the VideoAFM images is not simple to interpret. Previously we have suggested that the VideoAFM images consist of a combination of topographic (*z*) and slope ($\text{d}z/\text{d}x$) information, implying that a VideoAFM image could be synthesised from the conventional AFM topographic image through the use of

$$I_{\text{VAFM}} = A z_{\text{AFM}} + B \frac{\text{d}z_{\text{AFM}}}{\text{d}x}$$

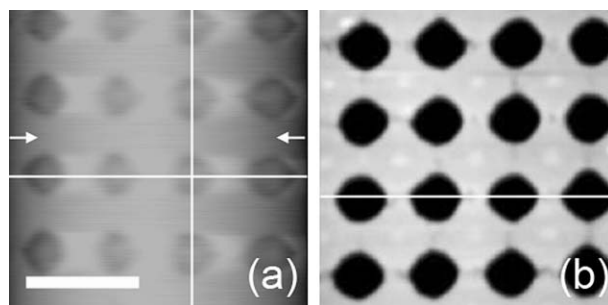


Fig. 1 (a) VideoAFM image, collected in 33.3 ms (15 frames s^{-1}), and the corresponding conventional AFM topographic image, (b), collected in 85 s, of a silicon oxide calibration grid. (b) Software zoom from a slightly larger (4 μm) image. The white horizontal and vertical lines indicate the position of line profiles shown in Fig. 3, the arrows indicate the position of the background line profile in Fig. 3. In (b) black to white represents a change in height of 45 nm. The scale bar represents 1 μm .

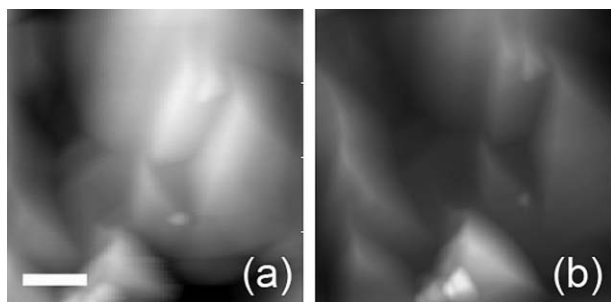


Fig. 2 (a) VideoAFM image, collected in 25 ms (20 frames s^{-1}) showing the surface of the quartz crystal tuning fork (micro resonator) that is the VideoAFM high speed scanner. (b) Conventional AFM image of the same area as (a), a software zoom from a slightly larger (5 μm) image. In (b) black to white represents a change in height of 200 nm. The scale bar represents 1 μm .

where I_{VAFM} is the pixel intensity in the VideoAFM image, z_{AFM} is the sample height as measured from the conventional AFM topographic image, x refers to the x -axis of the image, and A and B are (adjustable) parameters that define the relative contribution of edge and height effects to the VideoAFM image. Although this is approximately correct for surfaces in which the topography varies slowly (such as the quartz crystal surface shown in Fig. 2) it is not true when the surface includes sharper steps, such as those shown in Fig. 1. Here it is clear that relationship between the VideoAFM image and the true topography is not so simple, as is apparent from the difference in image contrast between the (in reality flat) areas between the holes down the edges of the image, and the topographically identical area in the middle of the VideoAFM image.

Fig. 3 shows a series of line profiles taken across the conventional AFM image, the same line in the VideoAFM image and a perpendicular line in the VideoAFM image. Here we will assume that the conventional AFM image is a true representation of the sample topography with the caveat that the topography measured is a convolution of the sample surface with the tip shape. The raw VideoAFM image, in contrast, appears considerably different from the topography. Even once a background, taken from the flat, hole free section of the sample surface, has been subtracted, additional features within the holes (arrowed) are seen that are not representative of the actual topography at that point. These are particularly clear in the orthogonal line section that is otherwise a truer representation of the sample surface. The VideoAFM image cannot be reconstructed from the conventional topographic image on a pixel by pixel basis, so a simple mapping of the VideoAFM image to the sample topography cannot be made. This combination of different contrast information occurs because the AFM cantilever is responding at a frequency considerably higher than its first bending mode. Rapid changes in topography will lead to greater changes in cantilever deflection (and therefore pixel intensity) than the same change in height but with a gentler slope, as in this latter case the length of the cantilever over which the bending is distributed is greater.

In the future we envisage using an interferometric method to determine the absolute position of the cantilever tip in the vertical (z) direction. Assuming the tip follows the sample surface, this approach should provide a VideoAFM image that

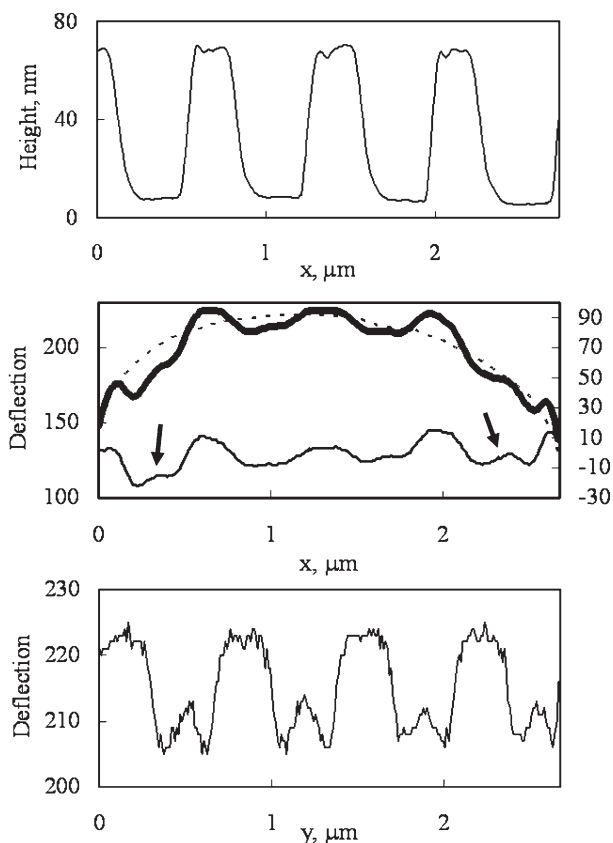


Fig. 3 A series of line profiles taken across the images shown in Fig. 1. (a) Taken across the conventional AFM image, Fig. 1(b), along the line shown. (b) The thick black line is taken across the horizontal line in Fig. 1(a), the dotted line is taken along the line indicated by the arrows in Fig. 1(a), and the thin black line is the dotted line subtracted from the thick black line. The arrows indicate regions of the profile that clearly do not correspond to the sample topography. (c) Line profile taken along the vertical line shown in Fig. 1(a), *i.e.* perpendicular to the fast scan axis of the microscope.

is a faithful representation of the sample surface. However, it should be noted that our current method, in which the deflection of the cantilever is monitored, gives an image in which the higher spatial frequencies are accentuated, so rapid variations in topography, on top of a slowly varying background, show up more clearly than they would in a true topographic image. For many applications, where what is required is a contrast mechanism that allows a feature of interest to be seen, this is an advantage when compared to a true topographic image.

The VideoAFM consists of both fast scan axis (through the micro resonator) and slow scan axis (through a conventional piezo). Thus an entire VideoAFM image can be obtained with the AFM cantilever stationary. Alternatively, the AFM cantilever can be scanned using the Dimension 3100 relative to the VideoAFM scanner and the image window provided by the VideoAFM moves around the sample surface. Fig. 4 shows an example of a composite image constructed from a series of VideoAFM images obtained by scanning the conventional microscope at a line rate of 0.1 Hz with 8 lines (trace and retrace) over an area of 10 μm . This composite image is

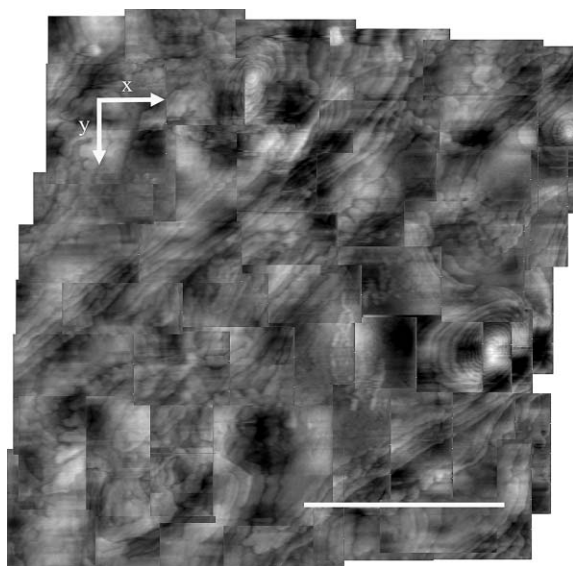


Fig. 4 A composite image made up from a series of VideoAFM images collected while scanning the cantilever relative to the VideoAFM scanner and sample over a 10 μm area using the conventional AFM scan tube. The sample is the surface of a polyethylene oxide thin film that has crystallized to form spherulites. The scale bar represents 5 μm .

approximately 1200×1200 pixels. The sample is a thin film of polyethylene oxide that has crystallized to form a spherulitic texture.¹⁹ The spherulite radius runs from bottom left to top right. Note that although the slow scan area is 10 μm , the actual area covered in Fig. 4 is somewhat larger due to the size of the VideoAFM images (this adds approximately 3 μm to the imaged area in each axis). Fig. 5 shows a conventional AFM image taken of the same area (256×256 pixels). The VideoAFM images are of a high quality and, although there are some variations in image contrast across images (*i.e.* from the edges to the centre) and between images, which results in the image edges remaining clear, the stitching of features between images is good. Although here the composite image was created by hand, it will be straight forward to automate this process. The composite image has a pixel resolution of 12 nm, compared with 59 nm in the conventional image.

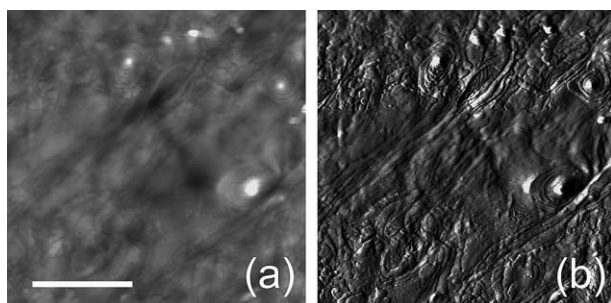


Fig. 5 A pair of conventional AFM images showing the area imaged in Fig. 4. (a) Topographic image, black to white represents a change in height of 250 nm. (b) Corresponding deflection image (the error signal from the feedback loop, that hence accentuates edges). The scale bar represents 5 μm .

Fig. 4 highlights one of the key advantages of the VideoAFM compared to conventional AFM and to other rapid scanning developments that use an approach more similar to that used in a conventional AFM^{11–12,14–16} or STM.¹³ In other approaches to fast scanning, the image rate is increased by increasing the rigidity of the scan stage (and hence its resonant frequency) and by miniaturising the cantilevers so as to increase their resonant frequency while reducing their inertia. This tends to lead to a maximum scan size of around 10 μm , and requires a complete redesign of the entire microscope. The VideoAFM uses a different approach. The use of a micro resonator as a scanner and cantilevers that are the same size as conventional cantilevers means that the VideoAFM scanner can be integrated with a large area conventional scan stage. This allows both high speed (video scanning) and conventional slow scanning of the same area, and also allows the high speed scan window to be moved around over the sample to build up high resolution images of large areas rapidly, a process we call ‘tiling’. This provides an image that has the ultimate resolution obtainable by the microscope, but of a relatively macroscopic area.

The composite image shown in Fig. 4 was collected relatively slowly (80 s) which compares to a maximum speed to cover the same area using the conventional AFM of approximately 270 s (assuming 30 s images of approximately 3 μm) if the same pixel resolution is to be obtained. However, here the slow scanning (fast tiling scan axis—marked x in Fig. 4) of the sample was carried out along the same axis as the fast scan direction of the VideoAFM, so the tiling speed had to be kept sufficiently slow to avoid significant shearing of the VideoAFM images. While collecting the data we also wished to be able to assess its quality in real-time by eye, which necessitated a relatively slow tiling speed. If the fast tiling axis was aligned parallel to the slow scan axis of the VideoAFM (*i.e.* along y in Fig. 4) the problem with image distortion would be minimized, as images would be elongated slightly, rather than sheared. In the limit, the slow scanner of the VideoAFM could be removed and the fast scan axis combined with a slow scan stage capable of moving over several 100 μm . In this case we envisage that an area of $100 \times 100 \mu\text{m}$ would be imaged with 10 nm lateral and sub-nanometre vertical resolution in approximately 20 s (assuming a resonant frequency of 20 kHz for the micro resonator and no overlap between images). It should be noted that the ensuing image would have 100 Mpixels.

Before discussing the wealth of possibilities that this large area, high resolution inspection opens up, it is worthwhile considering an alternative approach to rapid imaging. If the method for tracking the surface that we have developed for the VideoAFM was combined with a large area scanner capable of maintaining a comparable tip velocity ($\sim 15 \text{ cm s}^{-1}$) but only when imaging large areas (say 100 μm), would this be as effective an instrument? Indeed, for large area inspection, this might seem a more attractive proposition, as developing a scanner that could scan with a line frequency of $\sim 500 \text{ Hz}$ is probably possible and such an image would be more straightforward to process. However, there are several disadvantages of this approach. Firstly, the quality of the image depends on stability between lines—if there is any drift

in the vertical (z) position of the sample between lines then features become very difficult to discern, and accurate measurements become impossible. Secondly, a high line rate leads to a lower impact of inevitable mechanical noise. If there is mechanical noise with a frequency of tens of Hz, this will not significantly impact on the VideoAFM's ability to image features of nanometre dimensions. Such features are imaged in milliseconds. However, if the line rate is significantly slowed while maintaining the same tip-velocity, by increasing the line length, the time to traverse an entire feature in the slow scan direction is much greater. For example, for a 100 nm feature that needs to be traversed by 15 scan lines for an image to be obtained (assuming a line width of 10 nm, the lateral resolution of the AFM) the VideoAFM would image the feature in 0.75 ms (line rate 20 kHz) compared to 30 ms with the alternative approach (line rate 500 Hz).

The above discussion highlights the increased stability that scanning fast provides. Fig. 6 shows this effect to the full. The image is a tiled image similar to Fig. 4. However, in this case the image motion has been obtained by the motion of a conventional screw thread translation stage. The VideoAFM scan stage is mounted on a motorised x - y translation stage that is a standard part of the Dimension 3100 configuration for the coarse location of the sample over distances of up to 10 cm. In fact in this image the screw thread was turned by hand. Close examination of the image shows that stitching between the individual frames is still good. The reason for this remarkable stability is a simple by-product of fast scanning. The rapid response time of the cantilever that is necessary for a MHz pixel frequency means that sudden jolts provided by the course motion of the screw thread do not result in the cantilever leaving the sample surface. The high image rate means that only high frequency (10s of Hz) noise will cause distortion within an image, rather than between images, while if images are irretrievably damaged (for instance by the impulse when motion starts) there is sufficient over sampling of the surface to still construct an accurate composite image. We have found that, using a course translation stage, it is possible to traverse the entire 800 μm sample surface while still maintaining a real-time image of the surface with nanometre

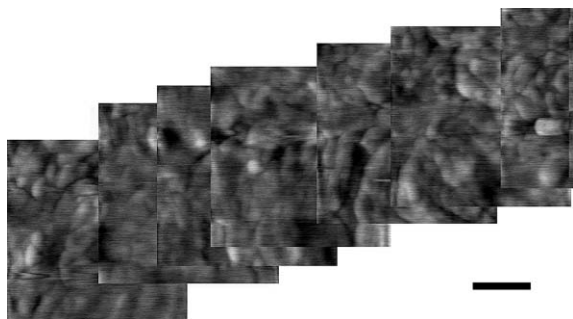


Fig. 6 A composite image made up from a series of VideoAFM images collected while the sample was being moved from right to left with a screw thread mechanical translation stage. The sample is the surface of a thin polyethylene oxide film that has crystallized to form a dendritic structure. The image on the left was collected first. Each VideoAFM image was collected in 33.3 ms (15 frames s^{-1}). The scale bar represents 1 μm .

resolution, in exactly the same way as would be done with a conventional optical microscope.

With any rapid scanning technique the maximum feature height that can be traversed is likely to be limited, and this is similarly true with the VideoAFM. However, the tiling technique outlined above provides a different approach to this issue. If the surface contains high features, but these features do not have sharp edges (an example of such a feature is a mammalian cell) it is possible to image them as a series of smaller tiles, in which the tile size is controlled so that the change in height within each image is within the range of the microscope.

In the above we have shown how the VideoAFM is capable of imaging both soft (*e.g.* polymeric) and hard (*e.g.* silicon) surfaces with high spatial resolution and 70 ms temporal resolution. We have also discussed the significant increase in image stability that a very high line rate gives, and how this allows us to manipulate the sample, while it is being imaged, using conventional mechanical means. We will now explore some of the future possibilities of the technique, and in particular how it might be expanded to allow the real-time analysis of surface properties at the nanometre scale.

As outlined in the Introduction, one of the strengths of AFM is that the mechanical interaction of the probe tip with the sample surface allows the measurement of mechanical properties of the surface and, through changes in these surface properties, the location of different chemical species on the sample surface can be determined. Currently we are only able to obtain topographical information with the VideoAFM and, as outlined above, this data has a complex relationship with the true topography of the sample surface. Clearly the potential applications of the technique would be greatly expanded if it were possible to obtain mechanical information relating to the surface. One possibility is to look at the lateral (*i.e.* frictional) interaction of the probe with the sample. As with the 'topographic' image, there may be significant problems in interpreting the data both because of the difficulties in separating the truly frictional from the topographical components of the lateral signal, but also because of the fundamental difference between the way in which the VideoAFM and a conventional AFM images. As discussed above, in a conventional AFM it can always be assumed that the cantilever is responding as a Hookeian spring, so the bending of the cantilever is simply related to the force applied to it. Similarly, the torsional motion of the cantilever is related to the torsional force through the torsional spring constant. However, in the VideoAFM the cantilever responds considerably faster than its first bending mode (*i.e.* its fundamental frequency)—the pixel frequency is $\sim\text{MHz}$, compared to a fundamental frequency $\sim 20\text{ kHz}$ —so there is no longer a simple relationship between force and cantilever deflection. Although the cantilevers are considerably stiffer torsionally than vertically, this still holds for frictional imaging, making direct measurement of frictional forces at these high frequencies problematic. However, we do believe that it will be possible to use this approach to image differences in the frictional interaction between adjacent areas in a sample, and by comparison between the lateral and vertical response of the cantilever some separation of topographic and frictional components will be obtained. It is hoped that this will lead

to one route to chemical analysis of surfaces with nanometre resolution at video rates.

An alternative approach is to make use of the very high rate at which data is collected and at which data can now be processed to map the mechanical properties of the sample surface. One of the parameters that can be controlled with the VideoAFM is the force applied to the surface, which is controlled electrostatically by varying the potential difference between a metal coating on the back of the cantilever and a ground plate beneath the sample. As this force, combined with the capillary force, is significantly greater than the force applied through the bending of the cantilever if the sample is relatively flat, VideoAFM images can be considered to be taken at approximately constant force. This is a good approximation if the roughness is below 10 nm. If consecutive images are taken of the same area but with a different applied force, then the difference between these two images will relate to the sample stiffness—the tip will indent soft areas more at high force than at low force, and will measure greater changes in topography between adjacent areas of different stiffness at high force than at low force. Real-time processing of such difference images would then give a surface map related to surface stiffness. This could, in turn, be related to the distribution of different materials across the surface (for instance in a composite material). We believe that this approach will allow the routine mapping of surface mechanical properties at near video rates with nanometre spatial resolution.

So far we have considered that capabilities of the VideoAFM as a surface analysis tool in its own right. Currently there is a much activity in the use of chemically patterned arrays for the analysis of biological molecules. Typically the patterning is carried out on the micron scale, and detection is performed optically through fluorescence. By shrinking the feature size in the array, the sensitivity of the device can be significantly increased.²⁰ However, once the period of the array becomes significantly smaller than the wavelength of light, fluorescence detection will no longer be possible (or at least not straight forward²¹). An alternative would be to use an AFM to measure changes in surface topography that occur when a binding event has taken place. In principle this could have sensitivity at the individual molecule level, as single proteins can be imaged with an AFM. The VideoAFM, with its ability to image large areas at high rates while maintaining nanometre resolution, will make this a real possibility. Indeed, it is conceivable that, through the use of SPM lithographic techniques,^{22,23} the same instrument could be used both to create, and ‘read-out’, an analytical device with molecular sensitivity.

Conclusions

VideoAFM is a new atomic force microscopy technique that provides true, video-rate images of a sample surface with nanometre resolution. The technique is applied to hard, silicon and quartz surfaces for the first time, and the ensuing images compared with those obtained conventionally. It is found that the VideoAFM image cannot be simply mapped onto the conventional image, as not only the height and slope of the surface effects the image, but also the frequency of surface

features as the cantilever is forced to respond at frequencies above its first resonant mode. It is suggested that the VideoAFM could measure true height with a displacement detection system (rather than bending detection system) such as an interferometer.

The integration of the VideoAFM within a conventional atomic force microscope allows large areas to be rapidly imaged with nanometre resolution by stitching together a series of VideoAFM images, a process dubbed ‘tiling’. When combined with the high stability that comes from a very rapid frame rate, it is possible to manually move the sample while imaging, allowing the true interaction of the user with the sample at the nanometre scale, in a manner akin to conventional, lens based, ‘far-field’²⁴ microscopes. This combination of capabilities opens up the possibility of rapid, nanometre resolution surface analysis over macroscopic areas.

Acknowledgements

We thank the Engineering and Physical Sciences Research Council for funding. Thanks also to Mr David Catto, Infinitesima, for instrument support.

References

- 1 G. Binnig, C. F. Quate and Ch. Gerber, *Phys. Rev. Lett.*, 1986, **56**, 930.
- 2 Y. Martin and H. K. Wickramasinghe, *Appl. Phys. Lett.*, 1987, **50**, 1455.
- 3 Y. Martin, D. W. Abraham and H. K. Wickramasinghe, *Appl. Phys. Lett.*, 1988, **52**, 1103.
- 4 R. W. Carpick and M. Salmeron, *Chem. Rev.*, 1997, **97**, 4, 1163.
- 5 A. Hammiche, L. Bozec, M. Conroy, H. M. Pollock, G. Mills, J. M. R. Weaver, D. M. Price, M. Reading, D. J. Hourston and M. Song, *J. Vac. Sci. Technol., B*, 2000, **18**, 3, 1322.
- 6 A. M. Chang, H. D. Hallen, H. F. Hess, H. L. Kao, J. Kwo, A. Sudbo and T. Y. Chang, *Europhys. Lett.*, 1992, **20**, 645.
- 7 A. Jauss, J. Koenen, K. Weishaupt and O. Hollricher, *Single Mol.*, 2002, **3**, 4, 232.
- 8 G. J. Leggett, N. J. Brewer and K. S. L. Chonga, *Phys. Chem. Chem. Phys.*, 2005, **7**, 6, 1107.
- 9 J. P. Cleveland, B. Anczykowski, A. E. Schmid and V. B. Elings, *Appl. Phys. Lett.*, 1998, **72**, 20, 2613.
- 10 F. Kienberger, G. Kada, H. Mueller and P. Hinterdorfer, *J. Mol. Biol.*, 2005, **347**, 3, 597.
- 11 T. Ando, N. Kodera, E. Takai, D. Maruyama, K. Saito and A. Toda, *Proc. Natl. Acad. Sci.*, 2001, **98**, 12468.
- 12 R. C. Barrett and C. F. Quate, *J. Vac. Sci. Technol., B*, 1991, **9**, 2, 302.
- 13 M. J. Rost, L. Schakel, E. van Tol, G. B. E. M. van Velzen-Williams, C. F. Overgaw, H. ter Horst, H. Dekker, B. Okhuijsen, M. Seynen, A. Vijftigschild, P. Han, A. J. Katan, K. Schoots, R. Schumm, W. van Loo, T. H. Oosterkamp and J. W. M. Frenken, *Rev. Sci. Instrum.*, 2005, **76**, 053710.
- 14 D. A. Walters, J. P. Cleveland, N. H. Thomson, P. K. Hansma, M. A. Wendman, G. Gurley and V. Elings, *Rev. Sci. Instrum.*, 1996, **67**, 3583.
- 15 T. Ando, N. Kodera, Y. Naito, T. Knoshita, K. Furuta and Y. Y. Toyoshima, *ChemPhysChem*, 2003, **4**, 11, 1196.
- 16 T. Sulchek, R. Hsieh, J. D. Adams, S. C. Minne, C. F. Quate and D. M. Adderton, *Rev. Sci. Instrum.*, 2000, **71**, 2097.
- 17 A. D. L. Humphris, M. J. Miles and J. K. Hobbs, *Appl. Phys. Lett.*, 2005, **86**, 034106.
- 18 A. D. L. Humphris, J. K. Hobbs and M. J. Miles, *Appl. Phys. Lett.*, 2003, **83**, 6.
- 19 H. D. Keith and F. J. Padden, *J. Polym. Sci.*, 1959, **39**, 101.
- 20 G. J. Leggett, *Analyst*, 2005, **130**, 3, 259.
- 21 V. Westphal and S. W. Hell, *Phys. Rev. Lett.*, 2005, **94**, 143903.
- 22 C. F. Quate, *Surf. Sci.*, 1997, **386**, 259.
- 23 S. Sun and G. J. Leggett, *NanoLett.*, 2004, **4**, 8, 1381.
- 24 C. Girard, C. Joachim and S. Gauthier, *Rep. Prog. Phys.*, 2000, **63**, 893.